

## Measurement of Large Distances in Biomolecules Using Double-Quantum Filtered Refocused Electron Spin–Echoes

Peter P. Borbat,<sup>†</sup> Jared H. Davis,<sup>‡</sup> Samuel E. Butcher,<sup>‡</sup> and Jack H. Freed<sup>\*†</sup>

Department of Chemistry and Chemical Biology, B52 Baker Lab, Cornell University, Ithaca, New York 14853, and  
Department of Biochemistry, University of Wisconsin-Madison, 433 Babcock Drive, Madison, Wisconsin 53706

Received February 4, 2004; E-mail: jhf@ccmr.cornell.edu

Double-quantum coherence (DQC)-ESR<sup>1,2</sup> has recently been shown to be a powerful technique for distance measurements in proteins.<sup>3</sup> It yields high-quality dipolar spectra, and it significantly extends the range of measurable distances in proteins with the use of double nitroxide labeling.<sup>4</sup> A previous study,<sup>3</sup> performed on T4 lysozyme mutants, demonstrated results covering distances between nitroxide labels of about 20–50 Å, which is a range accessible by pulse (but not cw)-ESR methods.<sup>1–6</sup> However, it is difficult to extend this range much beyond the 50 Å limit, because the acquisition time required to discern the dipolar oscillation (whose frequency is inversely proportional to the cube of the distance between the spin labels), becomes long compared to the electron-spin phase memory time,  $T_m$ . Whereas there are many potential mechanisms contributing to  $T_m$ , it was shown that for low temperatures (ca. 77 K) for labeled sites exposed to the frozen aqueous solvent, phase relaxation is largely (although not entirely) determined by nuclear spin diffusion of the matrix protons, which modulate their many-body dipolar interactions with the electron spin.<sup>3,5,7</sup> This yields a  $T_m$  for the primary echo of about 4 μs with a power law of  $n = 2$  as observed for T4 lysozyme in water–glycerol solutions (i.e. the decay goes as  $\exp[-(2\tau/T_m)^2]$ ).<sup>3</sup> The six-pulse DQC-ESR sequence utilized led to partial suppression of this mechanism of signal decay, because of its refocusing of the echo.<sup>2,3</sup>

In this communication we show how, by a variant of the DQC-ESR method, we are able to improve on the partial suppression of the effects of nuclear spin diffusion on the electron spin  $T_m$  and thereby to enable the accurate measurement of considerably larger distances, of about 70 Å. This variant employs the same six-pulse sequence, but in a format which simply refocuses the primary echo, after it is put through a double quantum filter. Thus, we refer to this method as double-quantum filtered refocused (DQFR)-electron spin–echoes (ESE). To demonstrate its use for long distances in biomolecules we studied a long double-stranded A-type RNA that was spin-labeled at both ends, consisting of 26 base pairs.<sup>8</sup>

3-(2-Iodoacetamido)proxyl spin label (Sigma) was attached to chemically synthesized RNAs containing a single 4-thiouracil at the 5' end (Dharmacon, Inc.), as previously described.<sup>9</sup> The reaction was monitored using UV spectroscopy at 320 nm as previously described.<sup>9</sup> Spin-labeled RNA was purified using a G-25 size exclusion chromatography column and complementary strands of labeled RNA were annealed by heating to 90° and slow cooling to room temperature. Complete 1:1 annealing of RNA was verified using non-denaturing polyacrylamide gel electrophoresis.

We show in Figure 1 the base-pair sequence, the spin-label moiety, and the molecular structure from molecular modeling. We estimate a distance of  $70 \pm 5$  Å between the two end labels.

The samples for ESR were about 100 μM in the doubly labeled RNA in 50 wt % D<sub>2</sub>O/glycerol-*d*<sub>8</sub>, with 200 mM NaCl and 20 mM Tris buffer at pH 7.5. The use of deuterated solvents is known to

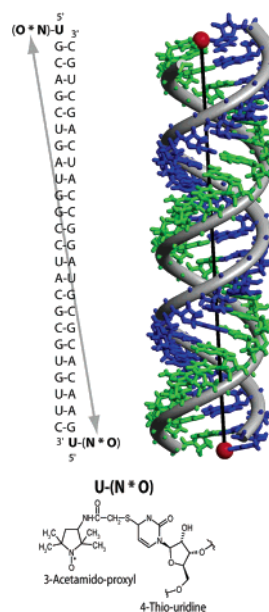


**Figure 1.** A-type, 26 bp RNA structure with the nitroxide label that is attached to 4-thiouridine shown. One strand is blue and the opposite green. Sites of spin-label attachments are shown as red spheres. Distance between them was measured to be 65 Å from the high-resolution X-ray crystal structure of an A-form duplex (PDB ID 1QCO) using Insight molecular modeling software (Accelrys). The flexibility of the linker arms may add 0–10 Å, depending on the relative positioning between spin labels.<sup>3</sup> Thus, we estimate the distance between spin labels to be  $70 \pm 5$  Å.

suppress the effects of nuclear-spin diffusion.<sup>5,7</sup> The sample size was about 10 μL, corresponding to about 1 nmole of doubly labeled RNA. The experiments were performed at 17.4 GHz, 6.2 kG, and 72 K, utilizing the home-built X/Ku-band 2D-FT-ESR spectrometer previously described<sup>10</sup> with a He-flow cryostat.

The six-pulse sequence arrangements for both DQC-ESR and DQFR-ESE are shown in Figure 2. In the limit of strong nonselective pulses the DQC-ESR signal yields the dipolar oscillations:  $-\sin at_p \sin at_2 = 1/2(\cos at_m - \cos at_\xi)$  where  $t_\xi = t_p - t_2$  and  $t_m = t_p + t_2$ , so the signal is displayed vs  $t_\xi$ . In the DQFR-ESE the equivalent expression for the signal is  $-\sin 2a\tau = 1/2(\cos 2a\tau - 1)$ , so the signal is displayed vs  $2\tau$ . [Here  $a = 2D(1 - 3\cos^2 \theta)/3$  with  $D = 3\gamma_e^2 \hbar / 2r^3$ , the dipolar spin–spin interaction.] The refocused echo varies with  $\tau$ , so simple relaxation due to  $T_2$  will yield a decay of  $e^{-4\tau/T_2}$  superimposed on the time-evolved signal (neglecting the small  $t_1$ ). The “zero deadtime” feature of DQC-ESR eliminates the decay due to  $T_2$ , instead replacing it by a constant reduction in the signal by  $\exp[-(2t_m/T_2)]$ . However, when relaxation mechanisms dominate, which decay exponentially with a higher power of  $t$  (i.e.,  $n > 1$ ), then this “zero-dead time” feature will not eliminate the decay so that it is desirable to maximize the suppression resulting from refocusing of the echo. In the case of DQC, the signal is reduced by the factor  $\exp[-\{(t_m + t_\xi)/T_m\}^n +$

<sup>†</sup> Cornell University.

<sup>‡</sup> University of Wisconsin-Madison.

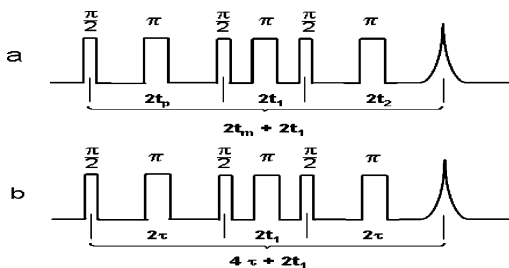


**Figure 2.** Six-pulse sequence used in (a) DQC ESR and (b) DQFR-ESE. In (a) one steps out  $t_p$  with constant  $t_m$  (and  $t_1$ ) such that the echo is always detected at the same period:  $2t_m + 2t_1$  yielding effective “zero-dead time”.<sup>1–3</sup> In (b) one steps out  $2\tau$  and detects the refocused echo at  $4\tau + 2t_1$ . In both cases  $t_1$  is kept short.  $\pi/2$  ( $\pi$ ) pulses were 3 (6) ns wide using a  $B_1$  of about 30 G.

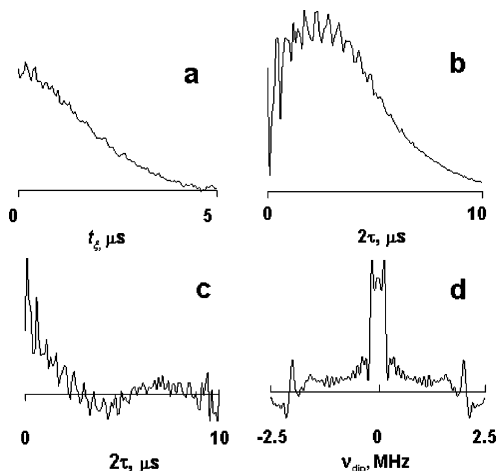


**Figure 3.** DQC ESR, (a) and DQFR-ESE (b) signal traces. DQFR-ESE signal (c) after removing relaxation decay and making standard linear baseline corrections,<sup>1–3,13</sup> and its Fourier transform (d). Signals were obtained at a 1 kHz data acquisition rate for 10 h.

$\{(t_m - t_g)/T_m\}^n$  for a decay mechanism depending on  $t^n$ .<sup>2,3</sup> In the case of DQFR the equivalent expression is  $\exp[-2(2\tau/T_m)^n]$ .

Let us consider these factors at the respective times  $t_{g,\text{Max}} = t_{m,\text{Max}}$  and  $2\tau = 2\tau_{\text{Max}}$  corresponding to the maximum acquisition times of these experiments, (wherein, e.g., each signal has reached the noise level). For comparable signals at these endpoints we find  $2\tau_{\text{Max}}/t_{m,\text{Max}} = 2^{(1-1/n)}$  (or  $2^{1/2} = 1.4$  for  $n = 2$  and  $2^{2/3} = 1.6$  for  $n = 3$ ). That is, one predicts a significant increase in the time available for observation of the dipolar oscillations for DQFR.

The DQC-ESR signal from the bilabeled 26 bp RNA of Figure 1 is shown vs  $t_g$  in Figure 3a. Data could be collected for a  $t_{g,\text{Max}} = t_{m,\text{Max}}$  of about 5  $\mu\text{s}$  as a result of effects of signal decay arising from nuclear spin diffusion. Over this time scale there is no discernible oscillation. The DQFR-ESE signal, obtained under identical conditions, is shown in Figure 3b. Here, it was possible to collect data until a  $2\tau_{\text{Max}}$  of about 10  $\mu\text{s}$ . Since this signal is also subject to  $T_2$  decay, its effect was removed by dividing by the refocused primary echo signal obtained using a weak pulse sequence with  $B_1 \approx 7.5\text{G}$  (thereby suppressing the dipolar oscillations, which require strong pulses). This also cancels the effects of nuclear spin diffusion and reduces effects of instantaneous diffusion.<sup>2,3</sup> (We estimate  $T_2 \approx 6 \mu\text{s}$  and an increased  $T_m \approx 7.5 \mu\text{s}$  due to solvent deuteration, with  $n = 2$  over a period of about 5  $\mu\text{s}$  then changing over to a decay with  $n \approx 3$ .) The resulting signal is shown in Figure 3c. It clearly displays the dipolar oscillation over the 10- $\mu\text{s}$  period. (The more rapid oscillations seen in Figure 3b and c are due to ESEEM effects<sup>11</sup> from nearby deuterons.) The Fourier transform of Figure 3c is shown in Figure 3d. A strong and clear dipolar

spectrum is obtained, corresponding to a dipolar splitting,  $\nu_{\text{dip}} = a = 140 \text{ kHz}$ . One may use the expression:  $r(\text{\AA}) = 37.3[\nu_{\text{dip}}(\text{MHz})]^{-1/3}$  to obtain the distance,  $r = 72 \pm 4 \text{\AA}$  between the end-labeled nitroxides<sup>3</sup> in excellent agreement with molecular modeling. Such a result could not have been reliably obtained from the DQC-ESR spectrum (although we were able to use DQC-ESR for a 16 bp end-labeled RNA corresponding to a distance of 55  $\text{\AA}$ ). The ESEEM spectral lines are well displaced on either side of the dipolar spectrum at  $\pm 2.0 \text{ MHz}$  or half the deuteron Larmor frequency (since the Fourier transform is with respect to  $2\tau$ ).

The DQFR-ESE method thus effectively extends DQC-ESR to longer distances by providing a longer interval of signal acquisition. We found approximately a doubling of this interval, which is actually greater than the theoretical estimate above. This might result from a better cancellation of other residual decay processes (e.g., instantaneous diffusion).<sup>2,3,5,12</sup> In addition, DQFR-ESE provides stronger signals vs  $\tau$  for the shorter  $\tau$ , (whereas in DQC-ESR one always collects data at time  $2t_m + 2t_1$ , for which there is substantial signal reduction, cf. above). But for distances  $\leq 50 \text{\AA}$  we do find DQC-ESR is preferable.<sup>14</sup>

Finally, we comment that, by retaining the DQ-filter and the use of short intense pulses, DQFR-ESE retains the virtues of DQC-ESR of (1) higher intrinsic sensitivity, since nearly all the spins may be irradiated, (2) the suppression of complications from correlations between orientations of the magnetic tensors of the nitroxide and the inter-radical vector, and (3) the filtering of undesirable artifacts. We do, however, give up the effective zero-deadtime feature as discussed and experience larger ESEEM, but this permits one to measure longer distances. DQFR-ESE is expected to be similarly useful for large distances between solvent-exposed sites in spin-labeled proteins.<sup>3</sup> However, when both spin labels are embedded within the soluble protein or within the transmembrane portion of a membrane-bound protein, then the shortened  $T_m$  due to surrounding protons (instead of solvent deuterons)<sup>2–4,7</sup> will significantly reduce the measurable range of distances, although the use of DQFR-ESE would still increase this range somewhat.

**Acknowledgment.** This work was supported by grants from the NIH/NICRR (J.H.F.) and NSF/Chemistry (J.H.F.) and by NIH Grant GM65166 (S.E.B.).

## References

- Borbat, P. P.; Freed, J. H. *Chem. Phys. Lett.* **1999**, *313*, 145–154.
- Borbat, P. P.; Freed, J. H. *Biol. Magn. Reson.* **2001**, *19*, 383–459.
- Borbat, P. P.; Mchaourab, H. S.; Freed, J. H. *J. Am. Chem. Soc.* **2002**, *124*, 5304–5314.
- Berliner, L. J.; Eaton, G. R.; Eaton, S. S., Eds. *Distance Measurements in Biological Systems*; Biological Magnetic Resonance, Vol. 19; Kluwer Academic: New York, 2000, provides extensive reviews of current ESR methods for distance measurements.
- Milov, A. D.; Maryasov, A. G.; Tsvetkov, Y. D. *Appl. Magn. Reson.* **1998**, *15*, 107–143.
- Pannier, M.; Veit, S.; Godt, A.; Jeschke, G.; Spiess, H. W. *J. Magn. Reson.* **2000**, *142*, 331–340.
- Huber, M.; Lindgren, M.; Hammarstrom, P.; Martensson, L. G.; Carlsson, U.; Eaton, G. R.; Eaton, S. S. *Biophys. Chem.* **2001**, *94*, 245–256.
- Schiemann, O.; Weber, A.; Edwards, T. E.; Prisner, T. F.; Sigurdsson, S. T. *J. Am. Chem. Soc.* **2003**, *125*, 3434–3435 have reported a 35  $\text{\AA}$  distance across an RNA duplex using nitroxide labels and PELDOR.
- Ramos, A.; Varani, G. *J. Am. Chem. Soc.* **1998**, *120*, 10992–10993.
- Borbat, P. P.; Crepeau, R. H.; Freed, J. H. *J. Magn. Reson.* **1997**, *127*, 155–167.
- Dikanov, S. A.; Tsvetkov, Yu. D. *Electron Spin—Echo Envelope Modulation (ESEEM) Spectroscopy*; CRC Press: Boca Raton, FL, 1992.
- Note that for our dilute 100  $\mu\text{M}$  solutions, corresponding to a mean distance of 255  $\text{\AA}$  between RNAs, instantaneous diffusion was weak and readily corrected for by standard methods. (cf. refs 3, 13)
- Jeschke, G.; Koch, A.; Jonas, U.; Godt, A. *J. Magn. Reson.* **2002**, *155*, 72–82.
- Existing PELDOR<sup>4–6</sup> (or DEER) techniques may usefully be applied to distances of 20–50  $\text{\AA}$ , but conditions of refocusing unfortunately lead to a decrease in the measurable distance range (cf. ref 6).

JA0493720